**Engineering Conferences International**
**ECI Digital Archives**

10th International Conference on Circulating Fluidized Beds and Fluidization Technology - CFB-10

Refereed Proceedings

2011

# Gas Tracer Study in a Non Mechanical L-Valve

Mohammad-Mahdi Yazdanpanah
*IFP, France*

Ali Hoteit
*IFP, France*

Ann Forret
*IFP, France*

Thierry Gauthier
*IFP, France*

Arnaud Delebarre
*ESSTIN, Universite Henri Poincare, France*

Follow this and additional works at: http://dc.engconfintl.org/cfb10

 Part of the Chemical Engineering Commons

## Recommended Citation

Mohammad-Mahdi Yazdanpanah, Ali Hoteit, Ann Forret, Thierry Gauthier, and Arnaud Delebarre, "Gas Tracer Study in a Non Mechanical L-Valve" in "10th International Conference on Circulating Fluidized Beds and Fluidization Technology - CFB-10", T. Knowlton, PSRI Eds, ECI Symposium Series, (2013). http://dc.engconfintl.org/cfb10/3

This Article is brought to you for free and open access by the Refereed Proceedings at ECI Digital Archives. It has been accepted for inclusion in 10th International Conference on Circulating Fluidized Beds and Fluidization Technology - CFB-10 by an authorized administrator of ECI Digital Archives. For more information, please contact franco@bepress.com.

# GAS TRACER STUDY IN A NON MECHANICAL L-VALVE

Mohammad-Mahdi Yazdanpanah[1], Ali Hoteit[1], Ann Forret[1*],Thierry Gauthier[1], Arnaud Delebarre[2]
[1] IFP Énergies nouvelles, Rond-point échangeur de Solaize- 69360 Solaize, France
*T: + 33 (0)4 37 70 20 00; F: +33 (0)4 37 70 20 08; E: Ann.forret@ifpen.fr
[2] ESSTIN, Université Henri Poincaré, Nancy, France

## ABSTRACT

A gas tracer (Helium) was used to study solid and gas flow in an L-valve. Effect of solid flow rate and pressure drop variation on the quantity of gas in the vertical section of the L-valve is presented. Results were then used to calculate the voidage of the moving solid bed in the L-valve vertical section.

## INTRODUCTION

The control of solid flow rate is an important element in many different solid circulating fluidized bed processes. The solid circulation control could be best achieved through use of the mechanical valves as in some mature catalytic process like FCC (1). However, use of the mechanical valves is more complex and limited in high temperature processes (>800°C) due to the material selection and resistance problem. Chemical Looping Combustion (CLC) is an example of this kind. CLC is a promising novel combustion technology involving inherent separation of the $CO_2$ (2). An oxygen carrier, mostly a metal oxide, transports oxygen from the air reactor to the fuel reactor while circulating between them. The solid transport rate controls the extent of reaction conversion in each reactor while controlling the energy balance in the system. The control of particles circulation rate is hence one of the most important factors in the CLC system.

The non-mechanical valves are a category of solid flow control devices employing no mechanically moving part (3). Accordingly, they can be easily adapted to high temperature conditions such as CLC. An external gas injection is used to control solid flow rate in these valves. L-valve is one of the possible choices for CLC process among different existing non-mechanical valves. It is simple in design, easy to operate, effective in solid flow control and requires minimum maintenance (4;5).

Various studies on the L-valve behavior have been published to date (3;5-9). These studies mostly illustrate the effect of operating and geometrical parameters on the solid flow rate actuated in the L-valve and the corresponding pressure drop (3;6-8). The flow in the horizontal section of the L-valve is an important subject in these studies. Three flow patterns have been distinguished in horizontal flow based on the aeration rate including: fast moving stream flow, dune-ripple flow, and dune-slug flow (5;7;9).

The solid flow in vertical section of the L-valve (standpipe) is in downwards cocurrent or counter current solid and gas flow. The particles flow in the dense

phase mode due to the gravity force. The pressure drop in this section is developed through the relative movement of gas and solid (3). As solids are not fluidized, change in the relative solid–gas velocity can change the pressure drop across the solid bed. Ergun equation (10) modified for slip velocities is used to calculate the pressure drop in the standpipe of the L-valve (3;7;11). Gas-solid flow in a standpipe can be largely divided into non-fluidized and fluidized flows. The non-fluidized bed flows are divided into the packed bed and the transitional packed bed flows by slip velocity (12). The slip velocity ($v_{sl}$) is defined as the interstitial gas velocity ($v_g$) minus the solid interstitial velocity ($v_s$) with downwards solid velocity as positive direction. Packed bed flow occurs when the interstitial slip velocity is positive and gas pressure is higher at the top of the standpipe than at the bottom. The bed porosity is believed to remain constant regardless of $v_{sl}$ value in this case (12). The transitional packed bed flow occurs when $v_{sl}$ is negative, and the gas pressure at the bottom of the standpipe is higher than that at the top (13). Different correlations have been developed to estimate the voidage of the solid bed in a standpipes. Some of the existing correlations in the literature are listed in Table 1.

Table 1: Correlations of solid bed voidage in a standpipe/ downcomer (εsp).

| Correlation | Condition | Reference |
|---|---|---|
| $\varepsilon_{SP} = \varepsilon_s + \frac{(\varepsilon_{mf} - \varepsilon_s)}{v_{mf}} v_{sl}$ | linear relation between gas velocity and voidage | Knowlton T. M. and Hirsan I. (3) |
| $\bar{\varepsilon}_{SP} = 1 - \frac{1-\varepsilon_s}{R}$<br>$R = 3.1(d_p \rho_s)^{0.5} \quad for \quad \frac{U}{U_t} < 0.0168\left(\frac{U_o}{U_t}\right)^{-0.6}$<br>$R = 23.94(d_p \rho_s)^{0.3}\left(\frac{U}{U_t}\right) \quad for \quad \frac{U}{U_t} > 0.0168\left(\frac{U_o}{U_t}\right)^{-0.6}$ | Sand particles<br>$d_p$ (503, 232, 90) µm<br>$\rho_s$(2818,2730,2365)kg/m$^3$ | Yagi (14) |
| $\varepsilon_{sp} = 0.6953\left(\frac{C_d}{C_{ds}}\right)^{-0.054}$, $\frac{C_d}{C_{ds}} = \frac{Ar}{18\mathrm{Re}_s + 2.7\mathrm{Re}_s^{1.687}}$<br>$\mathrm{Re}_s = \frac{d_p \rho_g}{\mu_g}\left(\pm\frac{Q_{sp}}{A} + \frac{\varepsilon_{sp}}{1-\varepsilon_{sp}} v_s\right)$ | Geldart group A Alumina/Hydrated alumina/ FCC catalyst<br>$d_p$ (34.11,46.66, 54) µm<br>$\rho_s$ (2770.4, 2037.4, 1760.9) kg/m$^3$ | Li et al. (15) |
| $\frac{\varepsilon_{sp}}{D^{0.4}} = 2.25\left(\frac{C_d}{C_{ds}}\right)^{-0.2}$, $\frac{C_d}{C_{ds}} = \frac{Ar}{18\mathrm{Re}_s + 2.7\mathrm{Re}_s^{1.687}}$ | Sand particles<br>$d_p$ (95) µm, $\rho_s$ (2260) kg/m$^3$ | Chan C. W. et al. (16) |

## EXPERIMENTAL SETUP

IFP EN and TOTAL are collaborating on an R&D project on CLC. A novel CLC design based on the interconnected bubbling fluidized beds was developed at IFP EN to build a 10 $kW_{th}$ pilot plant. The main concern was to insure an independent solid flow control, and to achieve minimum gas leakages between the air reactor and the fuel reactor. A cold prototype was constructed with identical geometrical dimensions as the hot 10 $kW_{th}$ CLC prototype. The system is schematically illustrated in Figure 1. Detailed explanation of the system and function of each section can be find elsewhere (17).

Helium was used to trace the gas flow in different L-valve sections. Helium flow rate

was controlled by means of a rotameters at fixed pressures fed from a bottle with 99.99% Helium purity. A Protec™ Helium Sniffer Leak Detector was used as the Helium measurement device. It is capable of detecting He sucked in the device though a sniffer line by means of a mass spectrometer. The Helium injection and detection points are illustrated in Figure 1. Silica sand was used as the solid in the current study. The properties of particles are listed in Table 2.

Table 2: Properties of sand particles used in this study.

| Property | Value |
|---|---|
| $\rho_s$ (kg/m$^3$) | 2650 |
| $d_s$ (µm) | 321 |
| $d_{50}$ (µm) | 334 |
| $U_{mf}$ (m/s) | 0.068 |
| $\varepsilon_{mf}$ | 0.514 |
| $\varepsilon_s$ (free settled) | 0.46 |
| $\varepsilon_{st}$ (tapped) | 0.40 |
| Φ (sphericity) | 0.76 |

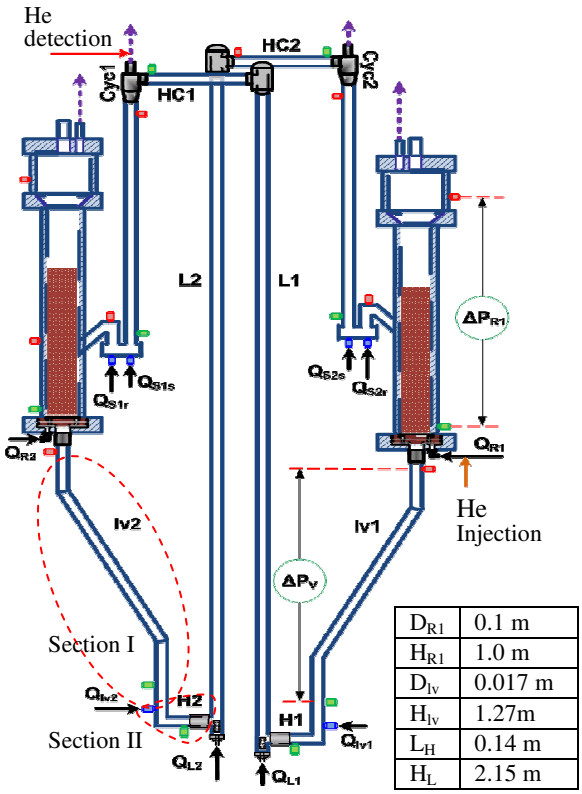


Figure 1: The scheme of the CLC cold flow prototype. Different Helium injection and detection positions are indicated in the figure.

## GAS TRACING IN THE L-VALVE

The gas and solid flow in two main sections of L-valve were experimentally investigated. The first section is the vertical part above the external gas injection point. Second section is the vertical section below external gas injection point together with elbow and horizontal pipe of the L-valve, (Figure 1). Tracer gas (Helium) was injected into the fluidization gas of the reactor with low concentration of 0.33 vol. %. Low inlet concentration of tracer gas was used to ensure that the tracer gas does not modify significantly properties of the fluidization gas (air). Helium was then detected in the cyclone gas exit (Figure 1).

Pressure drop in the standpipe ($\Delta P_v$) is a variable parameter that adjusts to match the pressure balance across the solid circulation loop. Change of $\Delta P_v$ will in turn change the quantity of gas passing through this section. Series of tests were conducted where the gas flow rate in the vertical section of the L-valve was measured for different pressure drops across the element. A unique feature of the current CLC installation is the possibility to adjust $\Delta P_v$ through variation of the pressure drop across the reactor ($\Delta P_R$) by change of the solid height in the reactor. This permits control of pressure drop across the standpipe independently from the L-valve external aeration.

The measurements were conducted during the steady state solid circulation for

different bed height in the reactor with constant external aeration rate in the L-valve ($Q_{lv}$). The superficial velocity of the gas and pressure drop in the vertical section of the L-valve are illustrated in Figure 2. Increase in $\Delta P_R$ causes the $\Delta P_v$ to reduce from +60 mbar to –30 mbar. The gas flow changes based on the pressure drop across the standpipe. Two zones can be distinguished for gas flow in the standpipe ($U_v$). In the case of high pressure drops in the standpipe, gas flows upwards in the standpipe and no Helium was detected in the gas exit of the cyclone (Cyc1 in Figure 1). As the pressure drop reduces below a critical value, gas starts flowing downwards in the standpipe and progressively increases as the pressure drop reduces further in the standpipe.

The variation of the interstitial velocities in the standpipe is illustrated in Figure 3 for the same tests series above. In the case of negative pressure drop, the slip velocity is positive and the gas velocity is higher than the solid velocity. As the pressure drop in the reactor increases, slip velocity reduces progressively to zero (the solid and the gas have the same velocity). At higher reactor pressure drops, the slip velocity becomes negative. In this case, the particles flow faster than the gas. Finally, the relative velocity increases more than the solid velocity in value, which means the gas flows upward in the standpipe in the opposite direction of the solids flow**.**

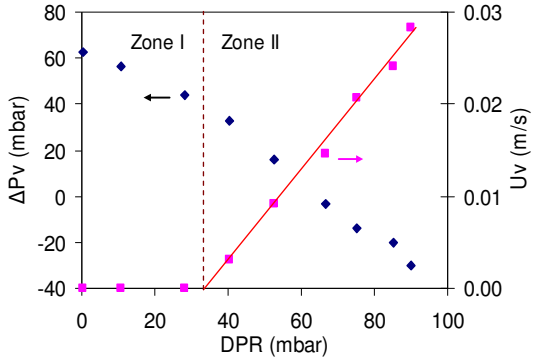


Figure 2: The effect of the reactor pressure drop on the pressure drop and the gas flow in the vertical section of the L-valve with $U_{lv}$ = 0.2 m/s.

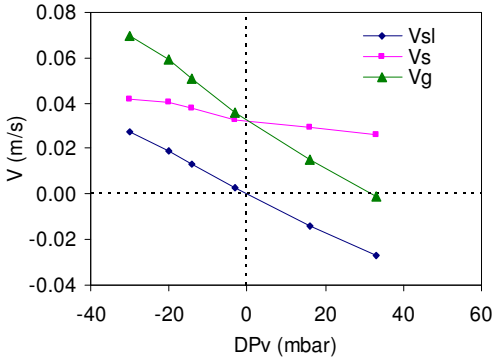


Figure 3: The change of the interstitial velocities in the standpipe due to the change of the standpipe pressure drop with $U_{lv}$ = 0.2 m/s and $G_s$ = 35 - 64 kg/m².s (equivalent to variation of $V_s$).

The variation of the gas flow through the vertical section of the L-valve changes the total gas flow around the bend of the L-valve. The solid flow rate in the L-valve is controlled by the gas flow rate through the bend of the L-valve ($Q_H$) (3). Therefore, the solid flow actuated in the L-valve will be affected due to the variation of the gas flow in the L-valve($U_V$). This phenomenon is shown in Figure 3 where increase of $\Delta P_v$ from -30 to 33 mbar reduces solid velocity from 0.042 to 0.026 m/s equivalent to solid flux variation of 64 to 43 kg/m².s.

The internal and the external L-valve air flow rates versus the solid flux in the L-valve are presented in Figure 4 for two test series. In the first series, the solid flow rate was controlled by the variation of the external L-valve aeration ($U_{lv}$). As expected, increase in $U_{lv}$ increases solid flux. Moreover, the gas flow rate in the standpipe increases as solids entrain more gases downwards in the standpipe. Gas

flow rate in the horizontal section of the L-valve which is sum of $U_{lv}$ and $U_v$ increases in the same order.

The external L-valve aeration ($U_{lv}$'), was kept constant in the second series of experiments presented in the Figure 4. The standpipe gas flow rate was then varied by adjusting the pressure drop across the standpipe through changes in the reactor pressure drop. Accordingly, for a constant external aeration, horizontal gas flow rate in the L-valve increases as $U_v$' increases. This demonstrate that for a constant external aeration of the L-valve, the solid flow rate can be varied through variation of the $U_v$ imposed by change of pressure drop across the standpipe. Therefore, the solid flow rate actuated in the L-valve is not only a function of the external aeration but also pressure drop across the L-valve. Knowlton (3;4;18) has explained this phenomenon being due to the fact that the solid flow rate in the L-valve is controlled by the quantity of the gas flowing around the bed of the L-valve ($Q_H$). This theory is well illustrated in the Figure 4 where the $Q_H$ curve lays on the same line for both of the experimental series. Standpipe gas flow variation is steeper in case of pressure drop change compared to the external aeration change for unit change of the solid flux. This is due to the fact that $Q_v$ must compensate required $Q_H$ variation for a unit change of solid flux while external aeration is constant.

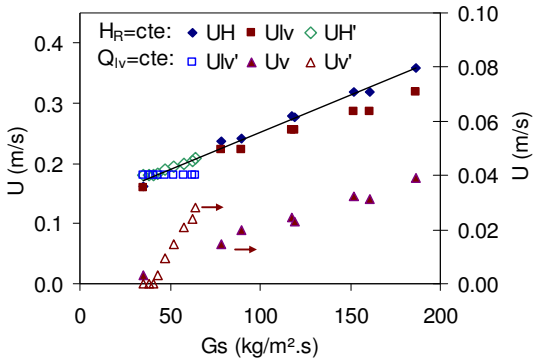


Figure 4: The variation of the solid flux versus the measured gas flow velocity in the L-valve for two experimental series: the change in external L-valve aeration with the fixed solid height (♦, ■, ▲) and the variation of the pressure drop in the standpipe with fixed external aeration (◊, □, Δ).

These results illustrate that a desired solid flow rate in the L-valve can be achieved by different configurations of the external aeration and the gas flow in the standpipe. This is of particular interest in case of CLC process where the gas flow out of the reactor is considered as a leakage and is desired to be minimized. Therefore, a proper control of pressure drop across the system together with appropriate external aeration helps to optimize this gas leakage out of the reactor.

## VOIDAGE OF THE MOVING SOLID BED

The experimentally measured pressure drop, gas flow rate and solid flow rate values were used to calculate the average voidage of the moving solid bed ($\varepsilon_{sp}$) based on the Ergun equation. As discussed before, the current installation permits to control the pressure drop across the standpipe independently from $Q_{lv}$. Using this feature, the voidage of the solid bed was measured for two non-fluidized solid flows regimes (Figure 5). The packed bed solid flow regime was reached when the pressure drop across the standpipe was negative, corresponding to positive slip velocities (see Figure 3). This corresponds to Zone II illustrated in Figure 5. The slip velocity is positive in this regime, as gas downward flow is faster than solids velocity (see Figure 3). The resulting moving bed voidage in this case is constant and corresponds roughly to the tapped bed voidage. In other words, gas flow pushes to

pack moving solids tighter together in this regime. Transition packed bed solid flow attained by imposing positive pressure drop in the standpipe. Slip velocities was negative in this region (see Figure 3). In this case, reactor pressure drop was kept constant and solid flow and pressure drop variation was adjusted through changes of $Q_{lv}$. Resulting variation of average voidage is illustrated in Figure 5, Zone I. Slip velocity is negative in this region, meaning that solid particles have higher velocity than gas. As slip velocity increases in value, voidage of solid bed expends from tapped bed voidage toward bed voidage at the minimum fluidization condition.

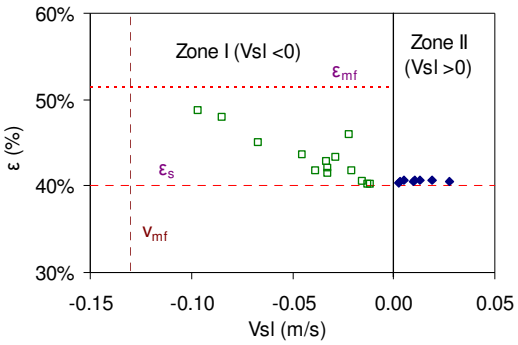


Figure 5: The experimental results of the variation of the average voidage of moving solid bed in the standpipe of the L-valve.

The correlations listed in the Table 1 were then compared with experimental results in Figure 6. Linear correlation proposed by Knowlton and Hirsan (3) results in closest prediction. Correlation of Li et al. (15) and Chan et al. (16) give a good estimate of the voidage variation trend, they however over/under estimates the voidage values. The significant difference observed in some cases is mostly due to different operating conditions in this test and developed correlations.

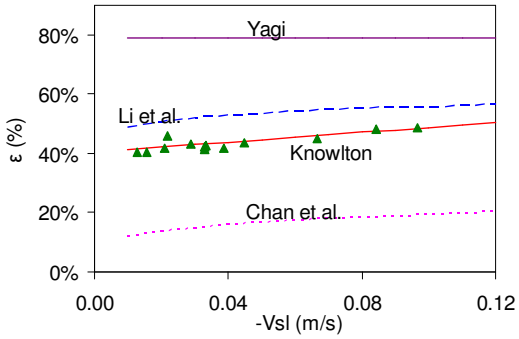


Figure 6: The experimental results of variation of the voidage of the moving solid bed in the standpipe of the L-valve compared with the literature correlations.

## L-VALVE LIMITING OPERATION

The L-valve operation is reported to be limited due to different limiting conditions including: fluidization of vertical arm (3), limit of solid flow rate into the L-valve (8), or unstable operation of the inclined section of the L-valve (19) (in case of hybrid standpipe as in the current configuration). However, these limits depend on the pressure drop across the standpipe of the L-valve which is a dependent variable parameter. Accordingly, the upper operation limit of the L-valve can be adjusted depending upon the operating conditions.

A test was carried out to investigate continuous operation of the L-valve in the limiting condition. External gas flow rate was set to a high value of 0.416 m/s. The resulting pressure drop variation and gas flow in the standpipe is illustrated in Figure 7. An oscillatory behavior of the pressure drop and gas the flow was observed in the system. Moreover, height of the moving bed in the standpipe was also behaving in an oscillatory mode. Once the L-valve was opened, solid height started to gradually decrease while pressure drop was increasing across the standpipe. The solid height finally got to a minimum level where it started to raise again. The solid height then increased till it reached the top of the L-valve where the solid height started to decrease again. This unsteady phenomenon repeated itself in an oscillatory mode

as illustrated in Figure 7.

When a very high gas flow rate is injected into the L-valve, a very high solid flow rate is actuated in the L-valve exit ($W_s$) higher than solid flow into the L-valve ($W_{in}$). The solid height in the standpipe ($H_s$) then reduces, resulting in increase of the pressure drop per unit height of the standpipe ($\Delta P/H_s$). Consequently, the downward gas flow rate in the standpipe ($U_v$) reduces gradually, get to zero and finally gas flows upwards in the standpipe. Accordingly, $U_H$ reduces, resulting in reduction of solid flow rate actuated in the L-valve. The solid inventory in the reactor then increases. Consequently, pressure drop in the reactor increases, resulting in reduction of the total pressure drop in the standpipe. As the solid flow rate reduces, $W_{in}$ exceeds $W_{out}$ and standpipe starts to fill. As the solid height in the standpipe increases, $\Delta P/H_s$ reduces. Therefore, more gas passes downwards, and the solid flow rate increases gradually. This continues until solid height gets its maximum once standpipe is filled with the solid and again $W_{out}$ exceeds $W_{in}$. Once more, the same cycle starts to repeat again. At the same time, the second L-valve (lv2 in Figure 1) was operating normally with an average solid flow rate equal to that of the first L-valve (lv1) which was operating in an unstable manner. The stable operation of the second L-valve was due to proper adjustment of the external aeration and the pressure drop along the standpipe. The external air flow velocity was set to 0.381 m/s (compared to 0.416 m/s in the lv1) and the pressure drop in the reactor was slightly higher in the reactor R2 compared to R1. This illustrates importance of proper selection of the operating conditions in high solid flow rate operations to avoid possible instable instabilities. This is of particular interest in the CLC process where a high solid circulation rate is desired between two reactors to transfer the required oxygen for combustion.

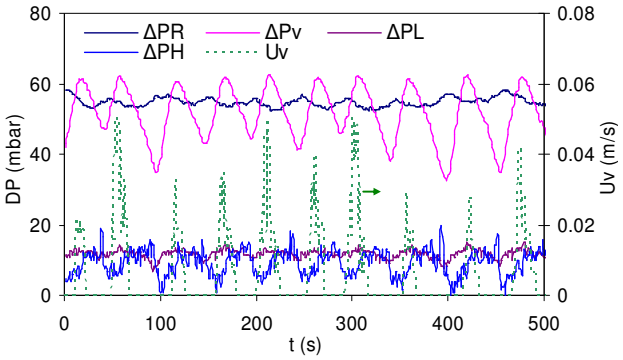


Figure 7: Oscillatory operation of L-valve in limiting condition of $U_{lv}$ = 0.416 m/s.

## CONCLUSION

The results of experimental study of an L-valve in a chemical looping combustion cold prototype was presented in this work. Helium was used as gas tracer to experimentally measure quantity of gas flow in the different sections of the L-valve. Gas flow rate in the vertical section of the L-valve increased by increasing solid flow rate or by decreasing pressure drop across the vertical section of the L-valve. Experimental results were then used to calculate the average voidage of the moving solid bed in the vertical arm of the L-valve. Voidage variation in two regimes of packed bed flow and transitional packed bed flow were presented. Finally, oscillatory operation of L-valve in the limiting condition was presented in terms of gas and solid flow and pressure drop.

## NOTATION

$G_s$: solid flux, kg/m².s.
$H_s$: Height of solid bed in the standpipe, m.
$V_g$: interstitial gas flow rate, m/s.
$V_s$: interstitial solid velocity, m/s.

$Q_{lv}$: The external L-valve aeration, $Nm^3/h$.
$U_{lv}$: external aeration flow velocity calculated based on the L-valve area, m/s.
$U_H$: gas flow velocity in the horizontal section of the L-valve, m/s.
$U_v$: gas flow velocity in the vertical section of the L-valve, m/s.
$V_{sl}$: gas-solid slip velocity, m/s.
$\Delta P_R$: pressure drop in the reactor, mbar.
$\Delta P_v$: pressure drop in he vertical arm of the L-valve, mbar.
$\varepsilon_s$: voidage of free settled solid bed.
$\varepsilon_{sp}$: voidage of solid bed in the standpipe.
$\varepsilon_{st}$: voidage of tapped solid bed.

## REFERENCES


1. Gauthier T., Bayle J., Leroy P. FCC: Fluidization Phenomena and Technologies. Oil & Gas Science and Technology - Rev IFP 2000;55(2):187.
2. Lyngfelt A., Leckner Bo, Mattisson T. A Fuidized-bed combustion process with inherent CO2 separation; application of chemical-looping combustion. Chemical Engineering Science 2001;56:3101.
3. Solids Flow Control using a Nonmechanical L-valve. Ninth Synthetic Pipeline Gas Symposium; Chicago, illinois. 1997.
4. Knowlton T.M. Feeding and Discharge of Solids Using Nonmechanical Valves. Institute of Gas Technology . 1988. Chicago, Illionois, Institute of Gas Technology.
5. Yang Wen-Ching, Knowlton Ted M. L-valve equations. Powder Technology 1993;77:49.
6. Chan CW, Seville J, Fan X, Baeyens J. Particle motion in L-valve as observed by positron emission particle tracking. Powder Technology 2009;193(2):137.
7. Geldart D., Jones P. The behaviour of L-valve with granular solids. Powder Technology 1991;67:163.
8. Smolders K, Baeyens J. The Operation of L-valve to Control Standpipe Flow. Advaced Powder technology 1995;6(03):163.
9. Yang TY, Leu LP. Multi-resolution analysis of wavelet transform on pressure fluctuations in an L-valve. International Journal of Multiphase Flow 2008;34(6):567.
10. Ergun S. Fluid flow through packed columns. Chemical Engineering Process 1952;48(2):89.
11. Smolders K, Baeyens J. The Operation of L-valve to Control Standpipe Flow. Advaced Powder technology 1995;6(03):163.
12. Kojabashian C. Properties of dense-phase fluidized solids in vertical downflow Massachusetts Inst. of Technology; 1958.
13. Zhang J.Y., Rudolph V. Transitional Packed Bed Flow in Standpipes. Can J of Chem Eng , 1991;69:1242.
14. Yagi S. Chemical Machinery, Japon 1952;16:307.
15. Li Y., Lu Y., Wang F., Han K., Mi W., Chen X. et al. Behavior of gas-solid flow in the downcomer of a circulating fluidized bed with a V-valve. Powder Technology 1997;91:11.
16. Chan C.W., Seville J., Fan X., Baeyens J. Solid particle motion in a standpipe as observed by Positron Emission Particle Tracking. Powder Technology 2009;194(1-2):58.
17. Yazdanpanah M.M., Hoteit A., Forret A., Delebarre A., Gauthier T. Experimental Investigations on a Novel Chemical Looping Combustion Configuration. OGST - Revue d'IFP Energies nouvelles 2010.
18. Wet and Dry Limestone Feeding Using an L-valve. Sixth International Conference on Fluidized Bed Combustion; Atlanta, Georgia. 1980.
19. Knowlton T.M. Standpipes and Nonmechanical Valves. In: Yang W-C, editor. Handbook of Fluidization and Fluid-Particle Systems. NEW YORK: MARCEL DEKKER, INC; 2003. p. 576.